Acta Astronautica 241 (2026) 199–206

Contents lists available at ScienceDirect

Acta Astronautica

journal homepage: www.elsevier.com/locate/actaastro

Research paper

Piecewise rational Padé and Hermite approximations for the elliptic Kepler equation

Manuel Calvo[1], Antonio Elipe[*], Luis Rández[1]

Universidad de Zaragoza, 50009 Zaragoza, Spain

ARTICLE INFO

Keywords:
Elliptic Kepler equation
Padé approximant
Hermite approximant
Rational interpolation
Orbital mechanics
Space trajectory analysis

ABSTRACT

Accurate and efficient solution of the Elliptic Kepler Equation (EKE) is fundamental in orbital mechanics and spacecraft trajectory analysis. In this work, we present a family of piecewise rational approximations for solving the EKE,

$$F(E;e) \equiv E - e\sin E = M,$$

based on Padé and Hermite-type formulations. The proposed approaches replaces the transcendental term $\sin E$ with Hermite and Piecewise Padé-Type (PPT) approximants, the later originally introduced by Brezinski, providing higher accuracy than the traditional Piecewise Padé (PP) method of Wu et al. without increasing computational cost. With these approximants, the resulting rational form reduces the EKE to a cubic equation that can be solved analytically, making it suitable for onboard implementations or large-scale orbit propagation tasks. Numerical experiments demonstrate that the PPT-based solution significantly improves accuracy for moderate and high eccentricities, including near-parabolic cases. Additionally, optimized parameter selection in general [3/2] rational representations yields further accuracy gains. These results show that the proposed piecewise rational method offers a reliable and computationally efficient alternative for precise orbital position determination across a wide range of eccentricities.

1. Introduction

The approximate solution of the elliptic Kepler's Equation (KE)

$$F(E;e) \equiv E - e\ \sin E = M \tag{1}$$

that defines uniquely the eccentric anomaly E of an elliptic orbit with eccentricity $e \in (0,1)$ as a function of the mean anomaly M has been the subject of research along several centuries [1,2].

A usual way for solving KE is based on non-linear iterative solvers such as Newton–Raphson or higher order methods [2–5] together with an optimal starter to guarantee the accuracy and the convergence of the solution of (1) with the minimum computational cost; see e.g. [6–10] and references therein.

An alternative approach to solve KE has been recently proposed by Philcox et al. [11]. By using a classical theorem in complex analysis [12] it is possible to express the solution of Eq. (1) for a given M as a quotient of two contour integrals along a Jordan curve of the complex plane that contains the unique real root corresponding to this M and no other zeroes of Eq. (1). A further improvement of this method is given in [13] by using ellipses as Jordan curves and by computing the quadratures by the composite trapezoidal rule.

A different approach to solve the KE consists in replacing the transcendental function $F(E;e)$ in Eq. (1) by a rational function $R(E;M,e)$ in E of type

$$R(E;M,e) = \frac{\alpha_0 + \alpha_1 E + \alpha_2 E^2 + \alpha_3 E^3}{1 + \beta_1 E + \beta_2 E^2 + \beta_3 E^3}, \tag{2}$$

with $\alpha_j = \alpha_j(M,e)$ and $\beta_j = \beta_j(M,e)$ so that the Eq. (1) is approximated by

$$R(E;M,e) = M, \quad \text{with} \quad M \in [0,\pi], \quad e \in (0,1) \tag{3}$$

that is equivalent to a cubic equation in the eccentric anomaly E and can be solved exactly by quadratures. Thus, Markley [3] by using a [3/2]-Padé approximation $\Omega(E)$ to $\sin E$ considers function $R(E;e) = E - e\,\Omega(E)$ that is of the type (2) and the solution of (3) refined by an additional iteration gives a highly accurate solution of (1).

* Correspondence to: Instituto Universitario de Matemáticas y Aplicaciones, Spain.
E-mail address: elipe@unizar.es (A. Elipe).
[1] Instituto Universitario de Matemáticas y Aplicaciones.

https://doi.org/10.1016/j.actaastro.2026.01.014
Received 15 October 2025; Received in revised form 19 December 2025; Accepted 4 January 2026
Available online 5 January 2026

Lynden-Bell [14] proposes as approximation of $F(E;e)$ a rational function in E of the type

$$R = R(E;M,e) = E - e\,E\left[\frac{1-E^2\,\phi_1}{1+E^2\,\phi_2}\right]\,\phi_3, \tag{4}$$

with suitable functions $\phi_1 = \phi_1(M)$, $\phi_2 = \phi_2(M,e)$ and $\phi_3 = \phi_3(M,e)$ obtained by imposing some requirements so that the solution of Eq. (3) with R given by (4) provides an accurate approximation to the exact solution of (1).

Mikkola [15] formulates KE in terms of the auxiliary variable $s = \sin(E/3)$ and then approximates by a cubic equation in s whose solution is a good approach to the solution of (1).

It is interesting to mention that the elliptic Kepler Eq. (1) for the limit eccentricity $e = 1$

$$F(E;1) = E - \sin E = M, \quad M \in [0,\pi], \tag{5}$$

is equivalent to the transcendental equation that appears in the homologous collapse radial evolution in time (see e.g. [16–19]) given by

$$x + \sin x = y, \quad y \in [0,\pi], \tag{6}$$

upon the changes $E \to \pi - x$, $M \to \pi - y$. Therefore, some results for the approximate solution of Eq. (6) can be applied also to the solution of KE (1).

In a recent paper [20], Wu and collaborators propose to take as rational function (2)

$$R(E;e) = E - e\,S(E), \tag{7}$$

where $S(E)$ is a piecewise [3/2]-Padé approximation of $\sin E$ in $[0,\pi]$. Then, the exact solution of (1), $E = E(M;e) = F^{-1}(M;e)$ is approximated by the exact solution of $R(E;e) = M$, that is, by $E_a = E_a(M;e)$ that can be obtained by solving a cubic equation. Additionally, the accuracy of E_a can be improved by one (or more) iterations of the Schröder method of suitable order.

The aim of this paper is two-fold. First of all we propose new Piecewise [3/2]-Padé-Type (PPT) approximants to $\sin E$ that are more convenient than the Piecewise Padé (PP) approximants considered by Wu et al. [20]. Recall that the so-called Padé-Type approximants [21, 22] have some flexibilities that do not have the pure Padé approximants that can be used to get C^1 continuity and better accuracy in our problem. Moreover, we observe that in solving KE with (7), our main target is not the accuracy of the approximation of $\sin E$, but the difference $F^{-1}(M;e) - R^{-1}(M;e)$ between the exact and the approximate solutions of KE. All these points will be considered in detail in Section 2.

Secondly, in Section 3 we study more general piecewise rational approximants that are defined by Hermite interpolants. This allows us a further improvement of the accuracy that will be confirmed with the results of numerical experiments.

Finally, in Appendix we show that the use of [3/3]-Padé or rational [3/3]-Hermite interpolations for the function $x - e\sin x$ is not recommended because there are singularities in the process of finding the coefficients.

2. Approximating the function $\sin E$ in KE by means of Padé approximant.

In this section we will use x instead of the eccentric anomaly E to connect with standard notations in approximation theory, $x = F^{-1}(M;e)$. To refine the meaning of Piecewise Padé (PP) approximant to the function $g(x) = \sin x$, with $x \in [0,\pi]$, we will say that $S(x)$ is a [3/2]-PP approximant of $g(x)$ if there exists a grid $\{s_j\}_{j=0}^{k}$ in $[0,\pi]$

$$0 = s_0 < s_1 < \cdots < s_k = \pi,$$

with $S(0) = g(0)$, $S(\pi) = g(\pi)$, and the restriction of $S(x)$ at each interval $(s_j, s_{j+1}]$ is the [3/2]-Padé approximant $S_{v_j}(x)$ of $g(x)$ at some base point $v_j \in [s_j, s_{j+1}]$. Hence, $S(x)$ is given by $S(0) = S(\pi) = 0$, and $S(x) = S_{v_j}(x)$ if $x \in (s_j,\, s_{j+1}]$ for $0 \le j \le k-1$.

Clearly the [3/2]-PP approximant depends on both the grid points s_j, $(1 \le j \le k-1)$, and base points v_j, $(0 \le j \le k-1)$. According to Brezinsky [21], if the approximant $S_{v_j}(x)$ at base point $x = v_j$, is defined by

$$S_{v_j}(x) = \frac{\sum_{\ell=0}^{3} \alpha_{j\ell}(x-v_j)^\ell}{1+\sum_{\ell=1}^{2} \beta_{j\ell}(x-v_j)^\ell}, \qquad x \in (s_j,\, s_{j+1}], \tag{8}$$

the six coefficients $\alpha_{j\ell}$ $(\ell = 0,1,2,3)$ and β_{jk} $(k = 1,2)$ of $S_{v_j}(x)$ are uniquely determined by the condition

$$S_{v_j}(x) - \sin x = \mathcal{O}\big(x - v_j\big)^p, \quad p \ge 6. \tag{9}$$

Because of the symmetry of $\sin x$ in $x \in [0,\pi]$ with respect to the midpoint $x = \pi/2$, Wu and collaborators [20] take $k = 5$ and select the base and grid points with the symmetry conditions

$$s_0 = 0, \quad s_j + s_{5-j} = \pi,\ (j = 0,1,2), \quad v_0 = 0, \quad v_j + v_{4-j} = \pi,\ (j = 0,1,2).$$

Hence, there are only three parameters $0 < s_1 < s_2 < \pi/2$ and $v_1 \in [s_1, s_2]$ to be chosen so that minimize the max error $\|\sin x - S(x)\|_\infty$ obtaining the values

$$s_1 = 0.536, \quad s_2 = 1.241, \quad v_1 = 0.890, \tag{10}$$

and then, the max norm $\|\sin x - S(x)\|_\infty \simeq 2.171 \times 10^{-6}$.

As remarked in [19] a drawback of the PP-approximant $S(x)$ with the parameters (10) is that it may have discontinuities at the grid points s_j, $(j = 1,\ldots,4)$ because

$$S_{v_{j-1}}(s_j) = \lim_{x \to s_j, x < s_j} S(x) \neq S_{v_j}(s_j) = S(s_j) \tag{11}$$

and these discontinuities are translated to the function $R(x;e) = x - eS(x)$, and therefore the equation $R(x;e) = M$ has no unique solution or even has no solution around the grid points s_j, $(j = 1,\ldots,4)$. This inconvenience is solved in [19] by using an alternative set of grid points $\widetilde{s}_j$

$$0 < \widetilde{s}_1 < \widetilde{s}_2 < \widetilde{s}_3 = \pi - \widetilde{s}_2 < \widetilde{s}_4 = \pi - \widetilde{s}_1 < \pi,$$

so that $S_{v_{j-1}}(\widetilde{s}_j) = S_{v_j}(\widetilde{s}_j)$ and then, the corresponding [3/2]-PP approximant $\widetilde{S}(x)$ associated to the new grid $\{\widetilde{s}_j\}_{j=0}^{k}$ has no discontinuities at the grid points and furthermore, $\widetilde{R}(x;e) = x - e\,\widetilde{S}(x)$ is monotonic increasing in $x \in [0,\pi]$ which guarantees that $\widetilde{R}(x;e) = M$ has a unique solution in x for all $e \in (0,1)$ and $M \in [0,\pi]$.

In this section we propose another alternative to overcome the discontinuity problem, it is the so-called Padé-Type approximants (PT) $\overline{S}_{v_j}(x)$ introduced by Brezinsky [21] and defined by

$$\overline{S}_{v_j}(x) = \frac{\sum_{\ell=0}^{3} \overline{\alpha}_{j\ell}(x-v_j)^\ell}{1+\sum_{\ell=1}^{2} \overline{\beta}_{j\ell}(x-v_j)^\ell}, \qquad x \in (s_j,\, s_{j+1}], \tag{12}$$

where the denominator can be arbitrarily chosen, although usually its coefficients $\overline{\beta}_{j\ell}$ are determined by imposing some conditions on the zeros or poles of $\overline{S}_{v_j}(x)$, and the coefficients $\overline{\alpha}_{j\ell}$ of the numerator are chosen so that $\overline{S}_{v_j}(x)$ attains the highest order of accuracy at $x = v_j$, that is,

$$\overline{S}_{v_j}(x) - \sin x = \mathcal{O}\big(x - v_j\big)^p, \quad p \ge 4. \tag{13}$$

With this condition, coefficients $\overline{\alpha}_{j\ell}$ are given by

$$\begin{aligned}
\overline{\alpha}_{j0} &= \overline{c}_{j0}\overline{\beta}_{j0},\\
\overline{\alpha}_{j1} &= \overline{c}_{j0}\overline{\beta}_{j1} + \overline{c}_{j1}\overline{\beta}_{j0},\\
\overline{\alpha}_{j2} &= \overline{c}_{j0}\overline{\beta}_{j2} + \overline{c}_{j1}\overline{\beta}_{j1} + \overline{c}_{j2}\overline{\beta}_{j0},\\
\overline{\alpha}_{j3} &= \overline{c}_{j1}\overline{\beta}_{j2} + \overline{c}_{j2}\overline{\beta}_{j1} + \overline{c}_{j3}\overline{\beta}_{j0}.
\end{aligned} \tag{14}$$

Table 1
Coefficients (12) of the [3/2]-PPT based at the same points s_i, ν_i as the PP one.

j	$\overline{\alpha}_{j0}$	$\overline{\alpha}_{j1}$	$\overline{\alpha}_{j2}$	$\overline{\alpha}_{j3}$	$\overline{\beta}_{j1}$	$\overline{\beta}_{j2}$	ν_j
0	0.00000000	−1.00000000	−0.00000000	−0.11628858	−0.00000000	0.05037808	0
1	0.77707174	−0.67457259	−0.29904036	−0.08462111	−0.05811634	0.06809716	0.89
2	1.00000000	−0.00000000	−0.41621151	−0.00000000	−0.00000000	0.08378848	$\frac{\pi}{2}$
3	0.77707174	−0.67457259	−0.29904036	−0.08462111	−0.05811634	0.06809716	$\frac{\pi}{2}$ −0.89
4	0.00000000	−1.00000000	−0.00000000	−0.11628858	−0.00000000	0.05037808	π

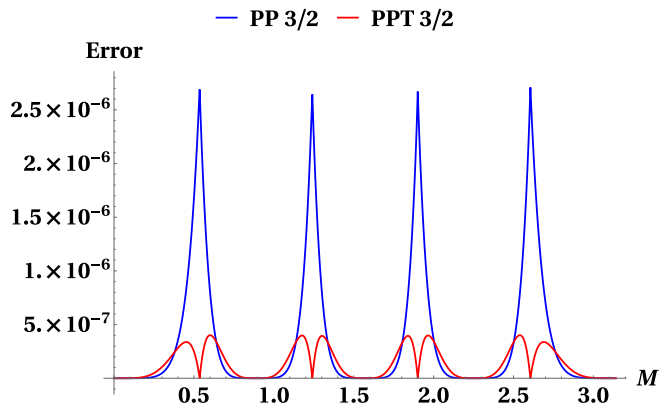

Fig. 1. Errors of the PP and PPT approximations to $\sin x$, based at the same points s_i, ν_i as the PP one.

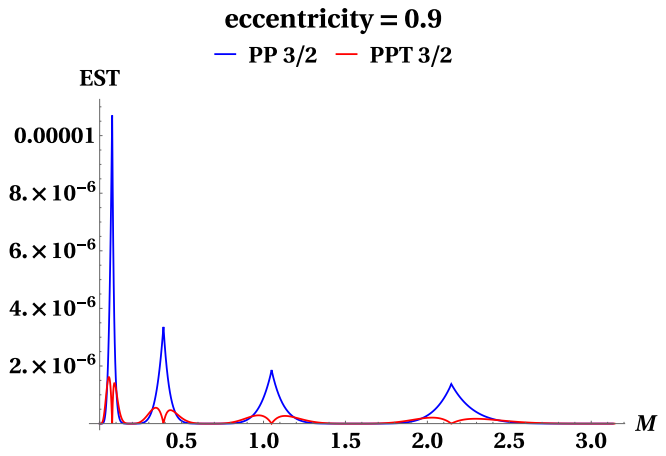

Fig. 2. Estimates (20) and (21) for $e = 0.9$ for all x_a and $\overline{x}_a$ in $[0, \pi]$ (i.e. $M \in [0, \pi]$).

where $\overline{c}_{j\ell}$, $(\ell = 0 \ldots)$ are the coefficients of the Taylor expansion of $\sin x$ at $x = \nu_j$,

$$\sin x = \sum_{\ell \geq 0} \overline{c}_{j\ell} (x - \nu_j)^{\ell}.$$

In our case, we choose $\overline{\beta}_{j1}$ and $\overline{\beta}_{j2}$ so that

$$\overline{S}_{\nu_j}(s_j) = \sin s_j, \quad \overline{S}_{\nu_j}(s_{j+1}) = \sin s_{j+1}, \tag{15}$$

i.e., the error of the PT approximant $\overline{S}_{\nu_j}$ of $\sin x$ be zero at both ends of the interval $[s_j, s_{j+1}]$. Hence the Piecewise Padé Type (PPT) approximant $\bar{S}(x)$ to $\sin x$ is defined by

$$\overline{S}(0) = \overline{S}(\pi) = 0, \quad \overline{S}(x) = \overline{S}_{\nu_j}(x), \quad x \in [s_{\nu_j}, s_{\nu_{j+1}}], \quad (j = 0, \ldots, 4) \tag{16}$$

that is continuous on the whole interval $x \in [0, \pi]$ and with null error at the grid points s_j.

There are still two free parameters to be chosen, one at the first subinterval $[s_0, s_1]$ and another one at the last subinterval $[s_4, s_5]$. In the first subinterval, in addition to fix the denominator of $\overline{S}_{\nu_0}$ to $\overline{S}_{\nu_0}(s_1) = \sin s_1$ we impose one additional order of accuracy at $x = 0$ due to the singularity of $\overline{R}(x; e)$ at $x = 0$ in the limit case $e = 1$. In the last subinterval $[s_4, s_5 = \pi]$, to fix the denominator of $\overline{S}_{s_5} = \overline{S}_{\pi}$, in addition to $\overline{S}_{\pi}(\pi) = \sin(\pi)$ we take the condition that the first derivtive be $\overline{S}'_{s_4} = \cos s_4$, i,e., a second order of accuracy at $x = s_4$. Note that the linear system (14) has a unique solution if $s_j < \nu_j < s_{j+1}$ (see Table 1).

With these conditions the PPT approximant $\overline{S}(x)$ to $\sin x$ is continuous, monotonic increasing and has no poles in $x \in [0, \pi]$.

In Fig. 1 we display the errors of the PP and PPT approximants to $\sin x$, $S(x)$ and $\overline{S}(x)$ given by

$$\mathbf{E} f(x) = \sin x - S(x), \qquad \overline{\mathbf{E}} f(x) = \sin x - \overline{S}(x)$$

As we can see, the max error of the PPT approximation is significantly smaller than the corresponding to the PP approximation. This is caused by the fact that in the PP approximation all coefficients of the S_{ν_j} are used to get the maximum accuracy at $x = \nu_j$ whereas, in the PPT approximation, the errors at the ends of each interval $[s_j, s_{j+1}]$ are null.

Another important point to be taken into account when comparing the quality of both approximants $S(x)$ and $\overline{S}(x)$ is the accuracy of the two algebraic equations

$$R(x; e) = x - e\, S(x) = M, \quad \text{and} \quad \overline{R}(x; e) = x - e\, \overline{S}(x) = M \tag{17}$$

in solving KE. Denoting by $x_{\text{exact}} = F^{-1}(M; e)$ the exact solution of KE corresponding to the mean anomaly M and eccentricity e by $x_a = R^{-1}(M; e)$ (respectively $\overline{x}_a = \overline{R}^{-1}(M; e)$), the solutions of the approximate Eqs. (17), these errors are

$$\Delta(x; e) = x_{\text{exact}} - x_a, \qquad \overline{\Delta}(x; e) = x_{\text{exact}} - \overline{x}_a. \tag{18}$$

Clearly the quality of the approximants $S(x)$ and $\overline{S}(x)$ of the function $\sin x$ should be evaluated by these errors.

To estimate the error $\Delta = \Delta(x; e)$ observe that

$$\begin{aligned} 0 &= F(x_{\text{exact}}; e) - R(x_a; e) = F(x_a + \Delta; e) - R(x_a; e) \\ &= F(x_a; e) - R(x_a; e) + \frac{\partial F}{\partial x}(x_a; e)\, \Delta + \mathcal{O}(\Delta^2), \end{aligned} \tag{19}$$

hence, an asymptotic estimate of Δ with order $\mathcal{O}(\Delta^2)$ is

$$EST(x_a; e) = \frac{-F(x_a; e) + R(x_a; e)}{\partial F / \partial x(x_a; e)} = \frac{e\left[-S(x_a) + \sin x_a\right]}{1 - e \cos x_a}. \tag{20}$$

Similarly for $\overline{x}_a$

$$\overline{EST}(\overline{x}_a; e) = \frac{-F(\overline{x}_a; e) + \overline{R}(\overline{x}_a; e)}{\partial F / \partial x(\overline{x}_a; e)} = \frac{e\left[-\overline{S}(\overline{x}_a) + \sin \overline{x}_a\right]}{1 - e \cos \overline{x}_a}. \tag{21}$$

Since errors and estimates both depend on the eccentricity, a comparison of the two approximants should be considered for the same eccentricity. In Fig. 2 we display the estimates (20) and (21) for $e = 0.9$ for all x_a and $\overline{x}_a$ in $[0, \pi]$ (i.e. $M \in [0, \pi]$). This figure shows that the PPT approximant gives smaller errors in the max norm than the PP approximant. A similar behavior is observed for other values of eccentricity.

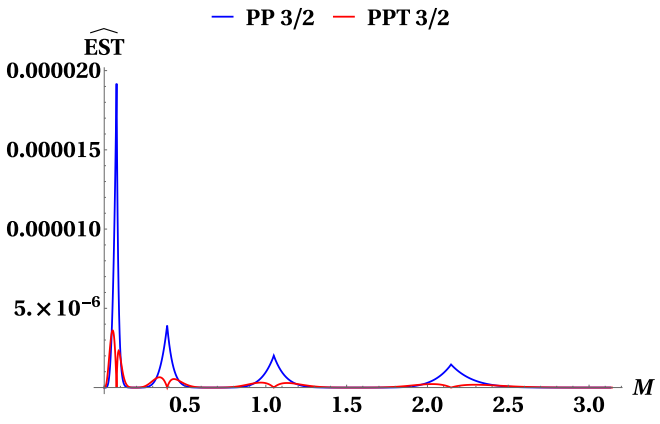

Fig. 3. Best upper bound of estimates given in Eqs. (22) and (23) for the [3/2]-PP and [3/2]-PPT aproximants.

To obtain an estimate of the error in the solution of KE that holds true for all values of eccentricity $e \in (0,1)$, observe that the function

$$\frac{\sin x - S(x)}{1 - e\cos x} \geq 0, \qquad x \in [0,\pi],\ e \in (0,1)$$

is a monotonic increasing function of x for all $e \in (0,1)$ hence, from (20) there follows that the best upper bound of $EST(x;e)$ is

$$\sup\{EST(x;e) \mid e \in (0,1)\} = \frac{\sin x - S(x)}{1-\cos x} \equiv \widehat{EST}(x), \tag{22}$$

and similarly for $\overline{EST}(x;e)$

$$\sup\left\{\overline{EST}(x;e) \mid e \in (0,1)\right\} = \frac{\sin x - \overline{S}(x)}{1-\cos x} \equiv \widehat{\overline{EST}}(x). \tag{23}$$

In Fig. 3 we display the upper bounds $\widehat{EST}(x)$ and $\widehat{\overline{EST}}(x)$ of the estimates for the PP and PPT approximants. Again, the error in the solution for all values of eccentricity in the case of the PPT approximant is better than the one corresponding to the PP approximant.

3. Piecewise rational Hermite interpolation

Another alternative to the piecewise [3/2]-Padé approximant $S = S(x)$ of the function $\sin x$, with $x \in [0,\pi]$, is to consider piecewise [3/2] rational Hermite interpolants $H = H(x)$. For a given grid $\{s_j\}_{j=0}^{p}$ in $[0,\pi]$, the piecewise Hermite interpolant $H = H(x)$ is defined in such a way that the restriction of $H(x)$ to the interval $[s_j, s_{j+1}]$, $(j = 0,\dots,p-1)$, denoted by $H_j(x)$, is a [3/2] rational function, where the coefficients are defined by a suitable Hermite interpolation of $\sin x$ in this interval $[s_j, s_{j+1}]$.

Since all $H_j(x)$ are [3/2] rational functions, they can be written in the form

$$H_j(x) = \frac{N_j(x)}{D_j(x)} \equiv \frac{\sum_{k=0}^{3} a_{jk}(x-s_j)^k}{1+\sum_{k=1}^{2} b_{jk}(x-s_j)^k}, \qquad (j = 0,\dots,p-1) \tag{24}$$

where the six coefficients $(a_{j0},\ a_{j1},\ a_{j2},\ a_{j3},\ b_{j1},\ b_{j2})$ are determined by imposing suitable Hermite interpolating conditions of function $\sin x$ in the interval $[s_j, s_{j+1}]$. These conditions will be defined with the auxiliary function

$$\Phi_j(x; a_{jl}, b_{jm}) \equiv N_j(x) - D_j(x)\,\sin x. \tag{25}$$

There are some requirements to be taken into account in this interpolation. First of all we want that $H = H(x)$ be continuous in $[0,\pi]$. Then, there must be

$$H_j(s_j) = \sin s_j, \ \text{ and } \quad H_j(s_{j+1}) = \sin s_{j+1}, \quad (j = 0,\dots,p-1). \tag{26}$$

By Eq. (24), this implies that $H_j(s_j) = a_{j0} = \sin s_j$, for $j = 0,\dots,p-1$, and $H_{p-1}(s_p) = \sin s_p$; therefore $H_0(s_0 = 0) = 0$ and $H_{p-1}(s_p = \pi) = 0$.

We also require that $H_j(x)$ has no poles in the intervals (s_j, s_{j+1}), i.e.

$$D_j(x) \neq 0, \quad x \in (s_j, s_{j+1}). \tag{27}$$

Moreover, because the function $F(E;e) = E - e\ \sin E$ is monotonic increasing in the variable $E \in [0,\pi]$ for all $e \in [0,1)$, it will be approximated by the algebraic function $R_H(E;e) = E - e\ H(E)$, with $R_H(0;e) = 0$ and $R_H(\pi;e) = \pi$.

Besides, we need that $R_H(E;e)$ be monotonic in $E \in [0,\pi]$, so that the approximate equation

$$R_H(E;e) = E - e\ H(E) = M \in [0,\pi] \tag{28}$$

has a unique solution, and this requirement holds iff

$$1 - e\ H_j'(x) > 0, \quad x \in [s_j, s_{j+1}], \quad \forall\, j = 0,\dots,p-1. \tag{29}$$

Taking into account the above requirements, (26), (27) and (29), we construct a piecewise Hermite interpolant for the symmetric grid used in [20], in order to make a comparison between both methods. For the first subinterval $[s_0 = 0, s_1 = 536/1000]$, due to the singularity of Kepler's equation for $E = 0$ and $e = 1$, we impose for the corresponding $H_0 = H_0(x)$ the six interpolating conditions at the endpoints of this interval

$$\begin{aligned} \frac{d^k H_0(s_0)}{dx^k} &= \left.\frac{d^k(\sin x)}{dx^k}\right|_{x=s_0}, \quad (k = 0,1,2,3), \\ \frac{d^k H_0(s_1)}{dx^k} &= \left.\frac{d^k(\sin x)}{dx^k}\right|_{x=s_1}, \quad (k = 0,1). \end{aligned} \tag{30}$$

In terms of the auxiliary function Φ of Eq. (25), the above conditions are equivalent to

$$\Phi_0^{(k)}(s_0) = 0,\ (k = 0,1,2,3), \quad \text{and} \quad \Phi_0^{(k)}(s_1) = 0,\ (k = 0,1),$$

a linear system of equations in the unknowns a_{0k}, $(k = 0,1,2,3)$, and b_{0m}, $(m = 1,2)$, which has a unique solution. Indeed, in the first interval $[0, s_1]$, the matrix of the coefficients of the linear system (30) is

$$\begin{pmatrix} 1 & 0 & 0 & 0 & 0 & 0 \\ 0 & 1 & 0 & 0 & 0 & 0 \\ 0 & 0 & 1 & 0 & e-1 & 0 \\ 0 & 0 & 0 & 1 & 0 & e-1 \\ 1 & 0 & -s_1^2 & -2s_1^3 & s_1^2(1-e\cos s_1) & -s_1^2(e\cos s_1 s_1 - 2s_1 + e\sin s_1) \\ 0 & 1 & 2s_1 & 3s_1^2 & e\cos s_1 s_1 - 2s_1 + e\sin s_1 & s_1(e\cos s_1 s_1 - 3s_1 + 2e\sin s_1) \end{pmatrix},$$

and its determinant is

$$\det(s_1) = e^2 s_1^2 \left(s_1 - \sin s_1\right)^2 \neq 0 \quad \text{if } s_1 > 0.$$

For the remaining subintervals $[s_j, s_{j+1}]$, $(j = 1,\dots,4)$, we take for $H_j = H_j(x)$ the conditions at three values of x, namely s_j, $s_j^* = (s_j + s_{j+1})/2$, and s_{j+1}:

$$\begin{aligned} \frac{d^k H_j(s_j)}{dx^k} &= \left.\frac{d^k(\sin x)}{dx^k}\right|_{x=s_j}, \quad (k = 0,1), \\ \frac{d^k H_j(s_j^*)}{dx^k} &= \left.\frac{d^k(\sin x)}{dx^k}\right|_{x=s_j^*}, \quad (k = 0,1), \\ \frac{d^k H_j(s_{j+1})}{dx^k} &= \left.\frac{d^k(\sin x)}{dx^k}\right|_{x=s_{j+1}}, \quad (k = 0,1). \end{aligned} \tag{31}$$

They are equivalent to

$$\Phi_j^{(k)}(s_j) = 0, \quad \Phi_0^{(k)}(s_j^*) = 0, \quad \Phi_j^{(k)}(s_{j+1}) = 0, \quad (k = 0,1), \tag{32}$$

again, these equations are linear in the unknowns a_{jk}, $(k = 0,1,2,3)$, and b_{jm}, $(m = 1,2)$, and for all $j = 1,\dots,p-1$, they have a unique solution because in the general case of an intermediate interval, e.g.,

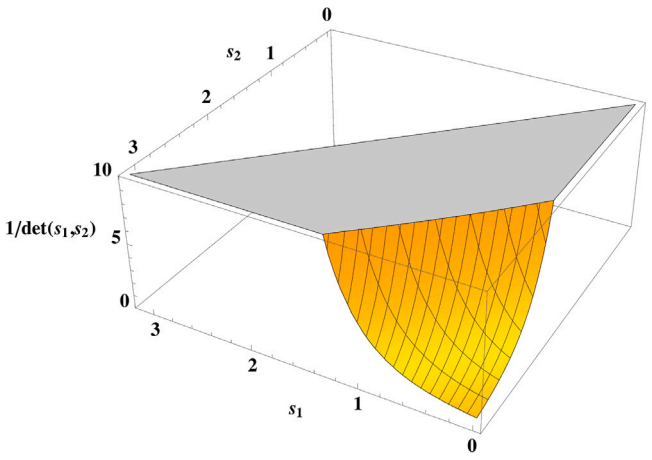

Fig. 4. The function $1/\det(s_1, s_2)$ for $0 < s_1 < s_2 < \pi$, is positive.

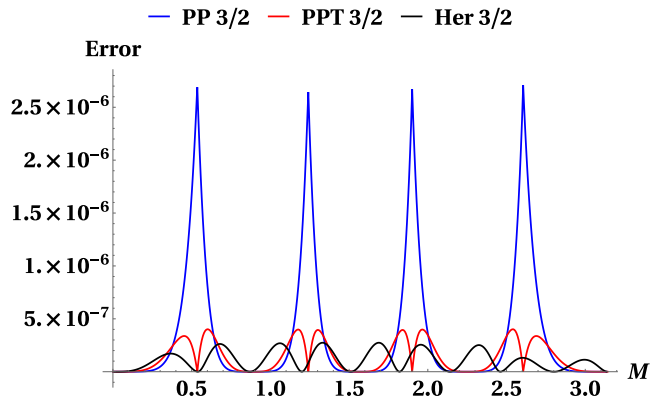

Fig. 5. Errors (ErrFun = $\sin x - H_j(x)$) of the PP, PPT and Hermite [3/2] approximations to $\sin x$.

$[s_1, s_2]$, after denoting $s^*_{12} = (s_1 + s_2)/2$, we get that the determinant of the matrix of the linear system (32) is not null. Indeed, the matrix is

$$\begin{pmatrix} 1 & 0 & 0 & 0 & 0 & 0 \\ 0 & 1 & 0 & 0 & -\sin s_1 & 0 \\ 1 & 0 & -\frac{1}{4} & -\frac{1}{4} & -\frac{1}{4}(s_1-s_2)\cos s^*_{12} & \frac{1}{8}\left((s_2-s_1)\cos s^*_{12} + 2\sin s^*_{12}\right) \\ 0 & 1 & 1 & \frac{3}{4} & \frac{1}{2}(s_1-s_2)\cos s^*_{12} - \sin s^*_{12} & \frac{1}{4}(s_1-s_2)\cos s^*_{12} - \sin s^*_{12} \\ 1 & 0 & -1 & -2 & (s_2-s_1)\cos s_2 & (s_2-s_1)\cos s_2 + \sin s_2 \\ 0 & 1 & 2 & 3 & (s_1-s_2)\cos s_2 - \sin s_2 & (s_1-s_2)\cos s_2 - 2\sin s_2 \end{pmatrix},$$

and its determinant

$$\begin{aligned} \det(s_1, s_2) = -\frac{e^2}{32} \quad & \Big(2(\sin s_2 - \sin s^*_{12})(3\sin s_1 - 4\sin s^*_{12} + \sin s_2) \\ & -(s_1 - s_2)\cos s_2 \left((s_1 - s_2)\cos s^*_{12} - 2\sin s_1 + 2\sin s^*_{12}\right) \\ & +(s_1 - s_2)\cos s^*_{12}(\sin s_1 - \sin s_2) \Big). \end{aligned} \tag{33}$$

It is not difficult to show graphically (Fig. 4) that if $s_1 < s_2$ (which is our case), then $\det(s_1, s_2) > 0$.

The above choice of Hermite's interpolant satisfies requirements (26), (27) and (29), i.e., the function $H = H(x)$ is continuous in $[0, \pi]$; $D_j(x) \neq 0$ for all $x \in [s_j, s_{j+1}]$, $(j = 0, \ldots, 4)$, and $1 - eH'(x) > 0$ for all $x \in [0, \pi]$ and $e \in [0, 1)$, as it can be easily checked.

Similarly, as the above case, in order to find an error estimate of the approximate solution with the piecewise Hermite interpolation (28), we proceed as in the previous Section 2, where we obtained the estimate of the error for the PPT approximant (21) just replacing $\overline{S}(x)$ by $H(x)$; then we have

$$\text{EST-Her}(E_a; e) = \frac{e\left(\sin E_a - H(E_a)\right)}{1 - e\cos E_a}, \tag{34}$$

where E_a is the solution of (28). Moreover, an upper bound of (36) for all values of $e \in [0, 1)$ is reached for $e = 1$, that is,

$$\overline{\text{EST-Her}}(E_a) = \frac{\sin E_a - H(E_a)}{1 - \cos E_a}. \tag{35}$$

To derive optimal coefficients for the Hermite approximation, we consider in the same way that before, five intervals, and the function to minimize is defined by

$$F(s_1, s_2, s_3, s_4) = \max_{\substack{i=1,\ldots,N,\\ k=1,\ldots,5}} \overline{\text{EST-Her}}\left(E_{a,k}\right),$$

where $E_{a,k}$ is computed at N equidistant points in $[s_{k-1}, s_k]$. that depends on the parameters s_1, s_2, s_3, s_4 with $s_0 = 0$, and $s_5 = \pi$.

The results of the computations for $N = 100$, are the following:

$$s_0 = 0,\ s_1 = 54/100,\ s_2 = 120/100,\ s_3 = 182/100,\ s_4 = 246/100,\ \text{and}\ \ s_5 = \pi.$$

For the above set of grid points s_j, the coefficients of the Hermite interpolant (24) are given in Table 2.

To compare the behavior of the new Hermite optimized interpolant with Padé and Padé Type approximants we display in Fig. 5 the errors ErrFun = $\sin x - H_j(x)$. We can see that the optimized Hermite approximnant appears to be the best approximant in the max norm.

We see that in the max norm, the accuracy of Hermite approximation is about one order higher than the corresponding Padé approximation, and twice the Padé type one. Clearly the Padé approximation is very accurate in a narrow neighborhood of the base point, but this accuracy rapidly decreases for points distant to the node; however, in Padé type and Hermite's approximations we may control the accuracy at several points of the interval.

In order to find an error estimate of the approximate solution with the piecewise Hermite interpolation (28), we proceed as in the previous Section 2 where we obtained the estimate of the error for the PPT approximant (21) just replacing $\overline{S}(x)$ by $H(x)$; then we have

$$\text{EST-Her}(E_a; e) = \frac{e\left(\sin E_a - H(E_a)\right)}{1 - e\cos E_a}, \tag{36}$$

where E_a is the solution of (28). Moreover, an upper bound of (36) for all values of $e \in [0, 1)$ is reached for $e = 1$, that is,

$$\overline{\text{EST-Her}}(E_a) = \frac{\sin E_a - H(E_a)}{1 - \cos E_a}. \tag{37}$$

We plot the errors in the KE solution when using three considered approximants (PP, PPT, Hermite) for eccentricities $e = 0.9$ and $e = 0.99$ in Figures Figs. 6 and 7 respectively.

The maximum of the estimate for the three approximants is presented in Fig. 8. There follows from the previous figure that the PPT and Hermite interpolants give similar error, and both are smaller than the Padé's approximant.

In Fig. 9 we plot the surfaces of the error of approximate KE solution with two different methods: (Top) The one of Wu et al. [20] that is a [3/2]-Padé with five intervals where the maximum of the error is 1.92×10^{-5}; (Bottom) The optimized [3/2]-Hermite with five intervals and max of error 3.17×10^{-6}. Hermite's approximant gives a one significative digit more than Padé's one, and besides, as we can observe in the figures, overall the behavior of Hermite's interpolant is better than Padé's one. Although we do not present here a plot for Padé type solution, its behavior is very similar to the Hermite one; for instance, the max error for PPT is 3.60×10^{-6}.

Table 2
Coefficients of the optimized [3/2]-Hermite interpolant.

j	a_{j0}	a_{j1}	a_{j2}	a_{j3}	b_{j1}	b_{j2}
0	0.00000000	1.00000000	−0.00041655	0.11551149	−0.00041655	0.05115517
1	0.51413599	0.86489922	−0.20991827	−0.08722295	0.01398569	0.06849942
2	0.93203908	0.32168494	−0.40407142	−0.00905898	−0.04363851	0.08351283
3	0.96910912	−0.34314753	−0.39182523	0.07263178	−0.09959169	0.07040895
4	0.63003062	−0.81935882	−0.22934429	0.11048430	−0.06791501	0.05231815

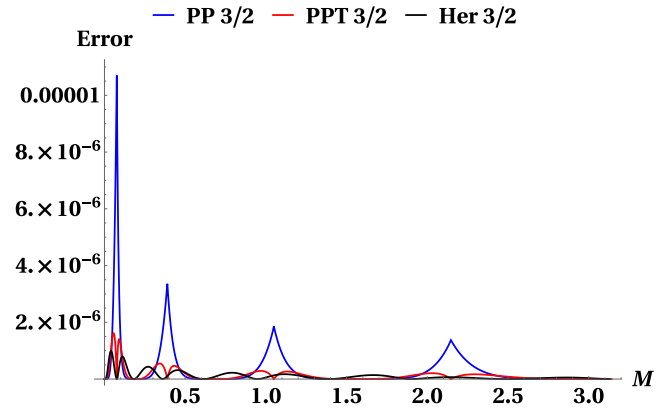

Fig. 6. Errors in the solution with the Padé (blue), Padé type (red) and Hermite (black) approximations in the interval $[0, \pi]$ for the eccentricity $e = 0.9$. (For interpretation of the references to color in this figure legend, the reader is referred to the web version of this article.)

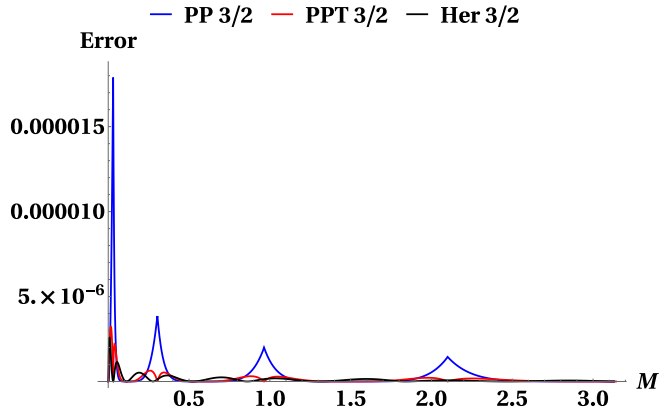

Fig. 7. Errors in the solution with the Padé (blue), Padé type (red) and Hermite (black) approximations in the interval $[0, \pi]$ for the eccentricity $e = 0.99$. (For interpretation of the references to color in this figure legend, the reader is referred to the web version of this article.)

4. Conclusions

In this work, we have introduced new Piecewise Padé-Type (PPT) approximations [21] for $\sin E$, which, when substituted into the transcendental Elliptic Kepler Equation (EKE),

$$F(E; e) \equiv E - e \sin E = M,$$

reduce it to a cubic polynomial equation solvable in closed form. By appropriately selecting the free parameters in the PPT denominators, the maximum-norm error of the approximate solution is significantly reduced compared with the traditional Piecewise Padé (PP) approximants of Wu et al. [20]. Numerical experiments confirm that PPT approximations yield substantially lower errors across the full range

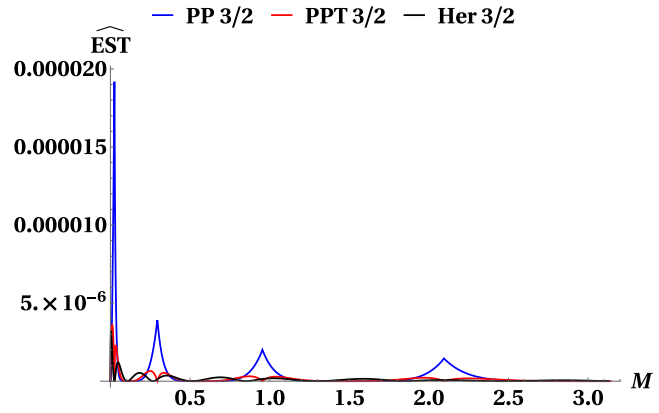

Fig. 8. Best upper bound of estimates given in Eqs. (22), (23), and (37) for the [3/2]-PP, [3/2]-PPT, and [3/2]-Hermite aproximants respectively.

of eccentricities $e \in (0, 1)$, with the greatest improvements observed for eccentricities approaching unity.

Furthermore, the use of more general piecewise [3/2] rational Hermite approximants to approximate $F(E; e)$ produces cubic equations whose solutions offer additional accuracy gains. Overall, this methodology provides a practical and computationally efficient approach for improving the accuracy of EKE solvers, particularly in applications requiring high-fidelity orbital position determination. The combination of PPT and rational Hermite approximants constitutes a versatile framework for precise and efficient orbital computations.

CRediT authorship contribution statement

Manuel Calvo: Writing – review & editing, Writing – original draft, Validation, Supervision, Methodology, Formal analysis, Conceptualization. **Antonio Elipe:** Writing – review & editing, Visualization, Validation, Supervision, Methodology, Formal analysis, Conceptualization. **Luis Rández:** Writing – review & editing, Validation, Supervision, Software, Methodology, Conceptualization.

Declaration of competing interest

The authors declare that they have no known competing financial interests or personal relationships that could have appeared to influence the work reported in this paper.

Acknowledgments

The authors are grateful to the anonymous reviewers for their constructive criticism and valuable suggestions, which significantly improved the original manuscript.

This work has been supported by Grants PID2022-141385NB-I00 and Proyecto PID2024-156002NB-I00 funded by MICIU/AEI/10.13039/501100011033/FEDER, UE and by the Aragon Government and European Social Fund (groups E24-26R and E41-26R).

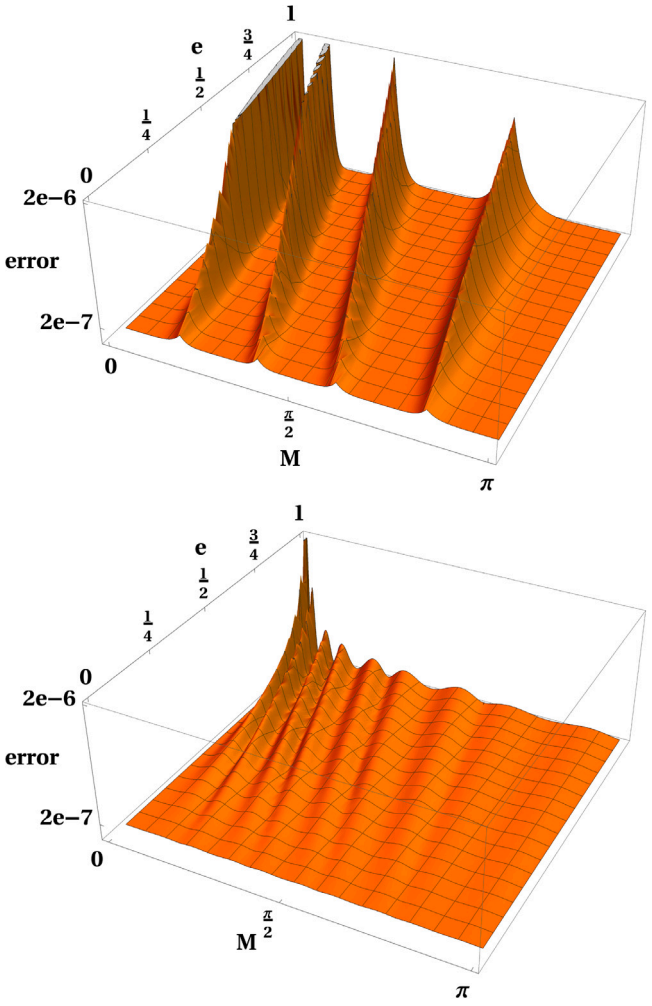

Fig. 9. Error in the domain $(e,\ M) = (0, 0.999) \times [0, \pi]$ for two approximations. (Top) The [3/2]-Padé proposed by Wu et al. [20] with five intervals. (Bottom) The optimized [3/2] Hermite with five intervals. We can observe that the later method is better than the former. To facilitate the comparison, we limit the error range to 2×10^{-6}.

Appendix. On the [3/3]-Padé or rational [3/3]-Hermite interpolations

For the problem studied, one may think to consider piecewise [3/3]-Padé or rational [3/3]-Hermite interpolations of the function $x - e \sin x$. However, this turned out to be not a good idea. Indeed, in the case of the [3/3]-Hermite, the interpolant $\widehat{H}(x)$ is given by

$$\widehat{H}(x) = \frac{a_0 + a_1 x + a_2 x^2 + a_3 x^3}{1 + b_1 x + b_2 x^2 + b_3 x^3};$$

the linear system in the coefficients a_i, b_i arising from the conditions of interpolation to the function $(x - e \sin x)$ corresponds to a matrix $\widehat{M}(s_j, s_{j+1}, e) \in \mathbb{M}_{7\times 7}$ which determinant has the expression

$$\det\big(\widehat{M}(s_j, s_{j+1}, e)\big) = e^2 \ \big(C_0(s_j, s_{j+1}) + e\, C_1(s_j, s_{j+1})\big)\,.$$

Therefore, if there exists a pair of values s_j and s_{j+1} such that the eccentricity $e^*(s_j, s_{j+1}) = -C_0(s_j, s_{j+1})/C_1(s_j, s_{j+1}) \in (0, 1)$, then $\det(\widehat{M}) = 0$ and the coefficients a_i, b_i of the [3/3]-Hermite interpolant are not defined.

In particular, if $s_{j+1} = \pi$ (i.e., in the last interval), it can be seen that for all $s_j < \pi$, there always exists a value of the eccentricity $e^* \in (0, 1)$ such that $\det\big(\widehat{M}(s_j, \pi, e^*)\big) = 0$. In fact, taking $s_j = \pi - a$, with $a > 0$,

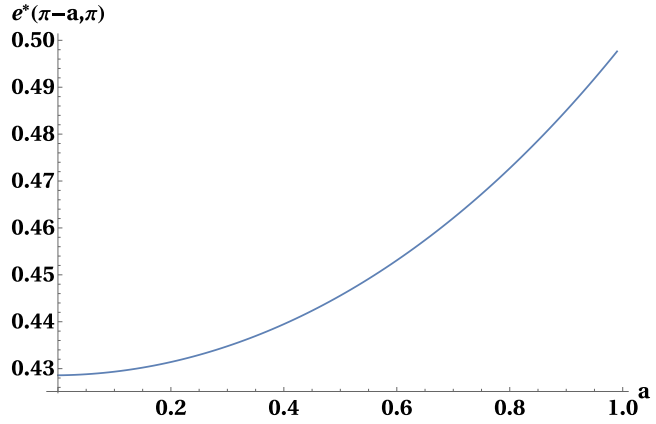

Fig. A.10. Plot of the $e^*(\pi - a, \pi)$ for $a \in [0, 1]$.

the matrix $\widehat{M}(\pi - a, \pi, e)$ is given by (where $\widehat{M}_i$ indicates the ith-row of $\widehat{M}$)

$$\begin{aligned}
\widehat{M}_1 &= \{1, 0, 0, 0, 0, 0, 0\}\\
\widehat{M}_2 &= \{0, 1, 0, 0, e\sin(a) + a - \pi, 0, 0\}\\
\widehat{M}_3 &= \Big\{ 1, 0, 0, \tfrac{1}{8}, \tfrac{-a^2}{16} e \sin(\tfrac{a}{2}), \tfrac{-a}{32}\big(ae\sin(\tfrac{a}{2}) + 4e\cos(\tfrac{a}{2}) + 4\big),\\
&\quad \tfrac{1}{64}\big((8 - a^2)e\sin(\tfrac{a}{2}) - 4(2ae\cos(\tfrac{a}{2}) + a + 2\pi)\big) \Big\}\\
\widehat{M}_4 &= \Big\{ 0, 1, 0, -\tfrac{3}{4}, \tfrac{e}{4}\big((a^2 + 4)\sin(\tfrac{a}{2}) + 2a\cos(\tfrac{a}{2})\big) + a\\
&\quad -\tfrac{\pi a}{8}\big(ae\sin(\tfrac{a}{2}) + 6e\cos(\tfrac{a}{2}) + 6\big),\\
&\quad \tfrac{1}{16}\big((a^2 - 12)e\sin(\tfrac{a}{2}) + 10\,ae\cos(\tfrac{a}{2}) + 4(a + 3\pi)\big) \Big\}\\
\widehat{M}_5 &= \Big\{ 0, 0, 1, \tfrac{3}{2}, \tfrac{-a}{4}\big(ae\sin(\tfrac{a}{2}) + 4\,e\cos(\tfrac{a}{2}) + 4\big), \tfrac{1}{8}(8 - a^2)e\sin(\tfrac{a}{2})\\
&\quad -a\,e\cos(\tfrac{a}{2}) - \tfrac{a}{2} - \pi,\\
&\quad \tfrac{1}{16}\big(24 - a^2)e\sin(\tfrac{a}{2}) - \tfrac{3}{4}(ae\cos(\tfrac{a}{2}) + 2\pi)\big) \Big\}\\
\widehat{M}_6 &= \{1, 0, -1, -2, a(e + 1), ae + a + \pi, ae + a + 2\pi\}\\
\widehat{M}_7 &= \{0, 1, 2, 3, -a(e + 1) - \pi, -a(e + 1) - 2\pi, -a(e + 1) - 3\pi\}.
\end{aligned}$$

In Fig. A.10 we plot the function $e^*(\pi - a, \pi)$ for $a \in [0, 1]$, and we can see that the values of the eccentricity $e^*(\pi - a, \pi) \in (0, 1)$, and therefore the matrix $\widehat{M}$ is singular.

Something similar happens for [3/3]-PP and [3/3]-PPT interpolations.

References

[1] P. Colwell, Solving Kepler's Equation over Three Centuries, Willmann-Bell, Richmond, VA, 1993, ISBN: 0943396409.

[2] R.H. Battin, An Introduction To the Mathematics and Methods in Astrodynamics, Revised ed., in: AIAA Educational Series, Reston, VA, ISBN: 978-1-60086-154-3, 1999.

[3] F.L. Markley, Kepler equation solver, Celest. Mech. Dyn. Astron. 63 (1995) 101–111, http://dx.doi.org/10.1007/BF00691917.

[4] A.W. Odell, R.H. Gooding, Procedures for solving Kepler's equation, Celest. Mech. 38 (1986) 307–334, http://dx.doi.org/10.1007/BF01238923.

[5] M. Palacios, Kepler equation and accelerated Newton method, J. Comput. Appl. Math. 138 (2002) 335–346, http://dx.doi.org/10.1016/S0377-0427(01)00369-7.

[6] M. Calvo, A. Elipe, J.I. Montijano, L. Rández, Optimal starters for solving the elliptic Kepler's equation, Celest. Mech. Dyn. Astron. 115 (2013) 143–160, http://dx.doi.org/10.1007/s10569-012-9456-5.

[7] M. Avendaño, V. Martín-Molina, J. Ortigas-Galindo, Solving Kepler's equation via Smale's α-theory, Celest. Mech. Dyn. Astron. 119 (2014) 27–44, http://dx.doi.org/10.1007/s10569-014-9545-8.

[8] M. Calvo, A. Elipe, J.I. Montijano, L. Rández, Convergence of starters for solving Kepler's equation via Smale's α-test, Celest. Mech. Dyn. Astron. 127 (2017) 19–34, http://dx.doi.org/10.1007/s10569-016-9713-0.

[9] A. Elipe, J.I. Montijano, L. L. Rández, M. Calvo, An analysis of the convergence of Newton iterations for solving elliptic Kepler's equation, Celest. Mech. Dyn. Astron. 129 (2017) 415–432, http://dx.doi.org/10.1007/s10569-017-9785-5.

[10] M. Calvo, A. Elipe, J.I. Montijano, L. Rández, A monotonic starter for solving the hyperbolic Kepler equation by Newton's method, Celest. Mech. Dyn. Astron. 131 (18) (2019) http://dx.doi.org/10.1007/s10569-019-9894-4.

[11] O.H.E. Philcox, J. Goodman, Z. Slepian, Kepler's goat herd: An exact solution to Kepler's equation for elliptical orbits, Mon. Not. R. Astron. Soc. 506 (4) (2021) 6111, http://dx.doi.org/10.1093/mnras/stab1296.

[12] D. Jackson, Non-essential singularities of functions of several complex variable, Ann. Math. 17 (1916) 172–179.

[13] M. Calvo, A. Elipe, L. Rández, On the integral solution of elliptic Kepler's equation, Celest. Mech. Dyn. Astron. 135 (2023) 26, http://dx.doi.org/10.1007/s10569-023-10142-7.

[14] D. Lynden-Bell, An approximate analytic inversion of Kepler's equation monthly notices of the royal astronomical society, 447, (1) 2015, http://dx.doi.org/10.1093/mnras/stu2326.

[15] S. Mikkola, A cubic approximation for Kepler's equation, Celest. Mech. 40 (1987) 329–334, http://dx.doi.org/10.1007/BF01235850.

[16] Z. Slepian, O.H.E. Philcox, A uniform spherical goat (problem): explicit solution for homologous collapse's radial evolution in time, Mon. Not. R. Astron. Soc.: Lett. 522 (2023) L42–L45, http://dx.doi.org/10.1093/mnrasl/slac153.

[17] M. Calvo, A. Elipe, L. Rández, On the numerical integration of an explicit solution of the homologous collapse's radial evolution in time, Mon. Not. R. Astron. Soc. 514 (2022) 1258–1265, http://dx.doi.org/10.1093/mnras/stac1418.

[18] Y. Zhou, B. Wu, C.W. Lim, H. Zhong, An approximate analytical solution for radial evolution of homologous collapse, Mon. Not. R. Astron. Soc. 522 (2023) 3278–3283, http://dx.doi.org/10.1093/mnras/stad1200.

[19] M. Calvo, A. Elipe, L. Rández, Approximate analytical solutions of the homologous collapse's radial evolution in time, Mon. Not. R. Astron. Soc. 533 (2024) 1986–1990, http://dx.doi.org/10.1093/mnras/stae1904.

[20] B. Wu, Y. Zhou, C.W. Lim, H. Zhong, A new solution approach via analytical approximation of the elliptic Kepler equation, Acta Astronaut. 202 (2023) 303–310, http://dx.doi.org/10.1016/j.actaastro.2022.10.049.

[21] C. Brezinsky, Padé-type approximation and general orthogonal polynomials, in: International Series of Numerical Mathematics, vol. 50, Birkhäuser-Verlag, Basel, ISBN: 3764311002, 1980.

[22] C. Brezinsky, M. Redivo-Zaglia, New representations of Padé, Padé-type and partial Padé approximants, J. Comput. Appl. Math. 284 (2015) 69–77, http://dx.doi.org/10.1016/j.cam.2014.07.007.